Title

Metal-Binding Isosteres as New Scaffolds for Metalloenzyme Inhibitors

Journal

Inorganic Chemistry, 57(15)

ISSN

0020-1669

Authors

Dick, Benjamin L

Cohen, Seth M

Publication Date

2018-08-06

DOI

10.1021/acs.inorgchem.8b01632

Peer reviewed

HHS Public Access

Author manuscript

Inorg Chem. Author manuscript; available in PMC 2019 August 06.

Published in final edited form as:

Inorg Chem. 2018 August 06; 57(15): 9538–9543. doi:10.1021/acs.inorgchem.8b01632.

Metal-Binding Isosteres as New Scaffolds for Metalloenzyme Inhibitors

Benjamin L. Dick and **Seth M. Cohen***

Department of Chemistry and Biochemistry, University of California, San Diego, La Jolla, California, 92093, USA

Abstract

The principle of isosteres or bioisosteres in medicinal chemistry is a central and essential concept in modern drug discovery. For example, carboxylic acids are often replaced by bioisosteres to mitigate issues related to lipophilicity or acidity, while retaining acidic characteristics in addition to hydrogen bond donor/acceptor abilities. Separately, the development of metal-binding pharmacophores (MBPs) for binding to the active site metal ion in metalloenzymes of therapeutic interest is an emerging area in the realm of fragment-based drug discover (FBDD). The direct application of the bioisostere concept to MBPs has not been well described or systematically investigated. Herein, the picolinic acid MBP is used as a case study for the development of MBP isosteres (so-called MBIs). Many of these isosteres are novel compounds and data on their physicochemical properties, metal binding capacity, and metalloenzyme inhibition characteristics are presented. The results show that MBIs of picolinic acid generally retain metal coordinating properties and exhibit predictable metalloenzyme inhibitory activity, while possessing a broad range of physicochemical properties (e.g., pK_a, LogP). These findings demonstrate the use of bioisosteres results in an untapped source of metal binding functional groups suitable for metalloenzyme FBDD. These MBIs provide a previously unexplored route for modulating the physicochemical properties of metalloenzyme inhibitors and improving their drug-likeness.

Graphical Abstract

*Corresponding Author: scohen@ucsd.edu (S.M.C.).

ASSOCIATED CONTENT

The Supporting Information is available free of charge on the ACS Publications website at DOI: 10.1021/acs.inorgchem.8b01632. Characterization and synthetic procedures for 4, 6, 7, 9, 12, 13, 14, 15, 18, 19, 20, 21, 22, and 23; crystallographic data and refinement details for all [(Tp^{Ph,Me})Zn(MBI)] complexes; figures of all [(Tp^{Ph,Me})Zn(MBI)] complexes; and tables of percent inhibition values against Endo and hCAII with standard deviations are provided in the Supporting Information. CCDC 1838692 – 1838705 contain supplementary crystallographic data for this paper. This data can be obtained free of charge via www.ccdc.cam.ac.uk/data_request/cif, by emailing data_request@ccdc.cam.ac.uk, or by contacting The Cambridge Crystallographic Data Centre, 12 Union Road, Cambridge CB2 1EZ, UK; fax: +44 1223 336033.

Conflict of Interest Statement

S.M.C. is a co-founder, has an equity interest, and receives income as member of the Scientific Advisory Board for Cleave Biosciences and is a co-founder, has an equity interest, and a member of the Scientific Advisory Board for Forge Therapeutics. Both companies may potentially benefit from the research results of certain projects in the laboratory of S.M.C. The terms of this arrangement have been reviewed and approved by the University of California, San Diego in accordance with its conflict of interest policies.

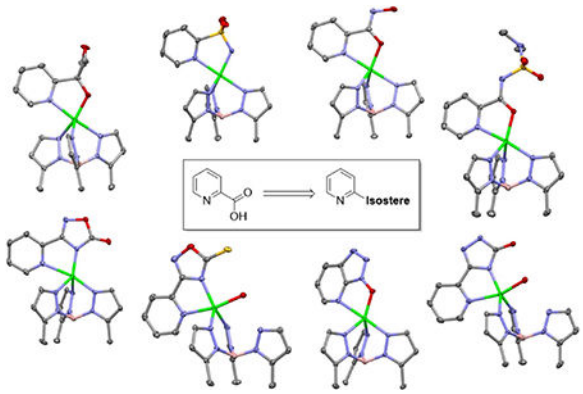

INTRODUCTION

The replacement of atoms or functional groups with an alternative atom or functional group with similar biological properties is known as isosteric or bioisosteric replacement.[1] Using isosteres (the terms isosteres and bioisosteres are used here interchangeably) to replace functional groups that possess liabilities, such as metabolic instability, poor solubility, low permeability, or even toxicity is a core concept in modern medicinal chemistry and critical for advancing lead compounds to clinically-effective therapeutics.[2] In a more pragmatic, but still important application, isosteres can also be used to help develop new chemical matter. For these and many related reasons, the application of isosteres is an essential tool in modern drug development, particularly for the carboxylic acid functional group.

Carboxylic acids are extremely important pharmacophores in bioactive compounds as is evidenced by their use in >450 drugs worldwide.[3] The ability of this functional group to engage in strong hydrogen bonding, electrostatic interactions, and metal coordination are key to its utility in bioactivce molecules. Despite its broad use, carboxylic acids are not without liabilities, which can range from poor membrane permeability to idiosyncratic toxicity.[4,5] One solution to this limitation is prodrugging carboxylic acids, often as esters;[6] however, a second solution is the use of isosteres. Recently, Ballatore and co-workers have highlighted the exceptional importance, success, and versatility of carboxylic acid isosteres.[7] In a valuable study, Ballatore reported on a series of phenylpropionic isosteres and compared these compounds across a range of physicochemical properties such as LogP, log$D_{7.4}$, pK_a, and others.[8] This thorough study demonstrated the broad range of carboxylic acid isosteres available and their physicochemical properties.

Fragment-based drug discovery (FBDD) is an important strategy that has proved very useful for the development of biologically active compounds,[9] including inhibitors of metalloenzymes.[10] The use of metal-binding pharmacophores (MBPs), which are small molecular fragments capable of binding metal ions, as privileged scaffolds for metalloenzyme targets has been reported.[11] These MBPs have been developed into highly active metalloenzyme inhibitors;[12–14] however, several of these MBPs contain carboxylic acids or free thiols which could have pharmokinetic liabilities. Herein, the concepts of MBPs and isosteres are combined to develop original metal-binding isosteres (MBIs) as a new class of compounds for FBDD. Using picolinic acid (**1**, Figure 1) as a representative

carboxylic acid containing MBP, we report 23 MBIs and explore their metal-binding properties, physicochemical properties, and metalloenzyme inhibitory activity against influenza H1N1 N-terminal PA endonuclease (Endo) and human carbonic anhydrase II (hCAII), both of which are metalloenzymes of clinical relevance. Like other isosteres, MBIs capture the potential to retain key properties of the pharmacophore (e.g., metal binding), while allowing for versatile and flexible modulation of physicochemical properties (e.g., pK_a, LogP). Although a relatively straightforward concept, the intimate and enabling combination of bioiniorganic and medicinal chemistry presented in these findings demonstrate that MBIs are a valuable and uncharted part of chemical space for developing innovative new pharmacophores for metalloenzyme inhibition.

METHODS SECTION

General Information.

Starting materials and solvents were purchased and used without further purification from commercial suppliers (Sigma-Aldrich, Alfa Aesar, EMD, TCI, etc.). Detailed syntheses of each MBI are provided in the electronic supporting information (ESI). [($Tp^{Ph,Me}$)ZnOH] ($Tp^{Ph,Me}$= hydrotris(5,3-methylphenylpyrazolyl)borate)) was synthesized as reported using [$Tp^{Ph,Me}$K], which was prepared as previously reported.[15] Absorbance and fluorescence activity assays were carried out using a BioTek Synergy HT plate reader.

Synthesis and Crystallization of TpZn(MBI) Model Complexes.

[($Tp^{Ph,Me}$)ZnOH] (150 mg, 0.27 mmol) was dissolved in 15 mL of CH_2Cl_2 in a 50 mL round bottom flask. The MBI (0.27 mmol, 1 equiv) in 10 mL of MeOH was added and the reaction mixture was stirred overnight under a nitrogen atmosphere. The resulting mixture was evaporated to dryness via rotary evaporation and subsequently dissolved in a minimal amount (~10 mL) of benzene. The solution was filtered to remove any undissolved solids. The resulting complex in benzene was recrystallized using vapor diffusion with pentane; crystals typically formed within 1 week.

Physicochemical Properties Analysis.

Physicochemical properties were determined using a Sirius T3 instrument. All titrations, both pK_a and LogP, were performed in 0.15 M KCl with 0.5 M HCL and KOH. The pK_a was determined by analyzing each MBI sample in triplicate using potentiometric or UV-metric titrations.[16,17] Experiments were typically performed over a pH range of 2.0 to 12.0. Standard deviations were derived from fitting all three replicate experiments.

LogP was determined via potentiometric titrations in the presence of varying ratios of octanol and water.[18] The presence of octanol shifts the pK_a of ionizable species and based on the shift a LogP can be determined. Measurements for LogP determination were typically performed over a pH range of 2.0 to 12.0. Three experiments with varying ratios of water:octanol were performed, allowing for a standard deviation to be determined from the fitting of all measurements. Using the measured pK_a and LogP values, $LogD_{7.4}$ was derived. MBI sample sizes were ≤0.5 mg for both pK_a and LogP measurements.

Endonuclease Assay.

Endonuclease was expressed and purified as previously reported.[13] The activity assays were carried in black Costar 96-well plates with a total volume of 100 μL per well. Assay buffer consisted of 20 mM Tris pH 8.0, 150 mM NaCl, 2 mM $MnCl_2$, 10 mM 2-mercaptoethanol, and 0.2 % Triton-X100. Endo was included at a final concentration of 25 nM and MBIs were added from a 50 mM DMSO stock to a final concentration of 200 μM. A fluorescent ssDNA-oligo substrate [([6-FAM]AATCGCAGGCAGCACTC[TAM]), FAM = 6-Carboxyfluorescein, TAM = tetramethylrhodamine] was used to monitor enzymatic activity. After addition of substrate, fluorescence (λ_{ex} = 485 nm, λ_{em} = 528 nm) was monitored over 45 min at 37 °C. Negative control wells contained no inhibitor and were set to 100% activity. A reported pyridinone based inhibitor was included as a positive control for inhibition.[13] Percent inhibition was determined by comparing the activity of wells containing MBIs to the activity of those without.

hCAII Assay.

The plasmid for recombinant expression of hCAII with a T7 RNA polymerase promotor and ampicillin resistance gene (pACA) was a gift from Thomas R. Ward (U. Basel, Switzerland). The protein for activity assays was expressed in BL21 *E. coli* cells and purified as reported previously.[19] Assays were carried out in clear-bottom Costar 96-well plates with a total volume of 100 μL per well. The assay buffer was comprised of 50 mM HEPES pH 8.0 and 100 mM $NaSO_4$. MBIs were added from a 50 mM DMSO stock to a final concentration of 200 μM and incubated with hCAII (100 nM final concentration) for 15 min at room temperature. *p*-Nitrophenyl acetate was used as the substrate (1 mM final concentration) and the absorbance at 405 nM was monitored for 20 min at 1 min intervals. Percent inhibition was determined by comparing the activity of wells containing MBIs to the activity of those without.

RESULTS AND DISCUSSION

MBI Design and Synthesis.

Picolinic acid (**1**, Figure 1) is a MBP that has been found to have activity against several metalloenzymes.[11] Inspired by recent work on the properties of carboxylic acid isosteres,[8] several MBIs of **1**, where the pyridinyl nitrogen coordination motif was maintained and the carboxylic acid group was varied, were prepared. A few previous studies utilizing isostere replacement for metalloenzyme inhibition have been reported, but they were limited to a small number of isosteres and provided little characterization beyond target inhibition data.[20,21] In designing MBIs, maintaining chelate ring size was prioritized, as it has a significant impact on the energetics of metal coordination. Therefore, the proposed MBIs (Figure 1) are designed such that they retain the ability to form a 5-membered chelate ring with a metal ion as is found for picolinic acid. Similarly, the MBIs were designed to retain the acidic character of the carboxylate. Maintaining chelate ring size and acidic ability were expected to be important in developing MBIs that would possess similar metal coordination and inhibitory activity as **1**.

Several of the MBIs were purchased from commercial vendors, including compounds **1**, **2**, **3**, **5**, **8**, **10**, **11**, **16**, **17**, and **24** (Figure 1). The remaining MBIs were synthesized starting from one of several pyridine precursors, including pyridine 1-oxide (**4**), 2-pyridine acid chloride (**6**), picolinic acid (**7**, **14**, **15**), methyl picolinate (**9**), 2-bromopyridine (**12**, **13**) 2-ethynylpyridine (**18**), 2-pyridinecarbonitrile (**19**), pyridine-2-carboxamide oxime (**20**, **23**), methyl picolinimidate (**21**), and pyridine-2-carboximidamide (**22**). The detailed synthetic procedures used to obtain these compounds and their complete characterization can be found in the Supporting Information.

Synthesis and Characterization of Model Complexes.

The metal binding mode of each isostere was evaluated utilizing a bioinorganic $Tp^{Ph,Me}Zn$ complex as a model system.[22] As the tridentate pyrazole ligand system closely resembles the coordination environment of a tris(histidine) metalloenzyme active site, it is a suitable system for a preliminary assessment of metal binding capability of MBIs. Our lab has previously reported the coordination complexes of compound **1**, namely [($Tp^{Ph,Me}$)Zn(**1**)] (Figure S1).[23] [($Tp^{Ph,Me}$)Zn(**1**)] shows that **1** binds in a bidentate fashion with the pyridine ring in an axial position and the carboxylate in an equatorial position, resulting in trigonal bipyramidal geometry. The crystal structure of **2** complexed to [($Tp^{Ph,Me}$)Zn] has also been reported,[24] showing the quinoline and hydroxyl group respectively coordinating in the same positions as pyridine and carboxylate groups of **1**.

Coordination complexes of [($Tp^{Ph,Me}$)Zn] were successfully obtained with several MBIs including, **3**, **5**, **7**, **9**, **11**, **12**, **15**, **17**, **18**, **19**, **20**, **21**, **23**, and **24**. In all obtained complexes, bidentate coordination to the Zn^{2+} ion was observed with the pyridine in the axial position and the carboxylic acid isostere occupying an equatorial coordination site (Figure 2, Figures S2 - S15). Both noncyclic (**3**, **5**, **7**, **9**, **11**, **12**, **15**) and cyclic (**17**, **18**, **19**, **20**, **21**, **23**) carboxylic acid isosteres, maintained the coordinative ability of the carboxylate upon its replacement. Fused ring systems also demonstrated similar coordination, with retention of the 5-membered chelate ring in [($Tp^{Ph,Me}$)Zn(**24**)]. All MBIs behaved as monoanionic ligands resulting in neutral [($Tp^{Ph,Me}$)Zn(MBI)] complexes. Overall the crystallized [($Tp^{Ph,Me}$)Zn(MBI)] complexes were similar to the [($Tp^{Ph,Me}$)Zn(**1**)] complex, with some interesting trends and slight differences being observed.

The noncyclic MBIs achieved bidentate coordination to the Zn^{2+} through the pyridine ring and a deprotonated oxygen donor atom, except for **5**, which exhibited bidentate coordination through the pyridine ring and a deprotonated sulfonamide nitrogen (Figure 2). For the noncyclic isosteres, the [($Tp^{Ph,Me}$)Zn(MBI)] complexes revealed that oxygen donor atoms were favored for coordinating the Zn^{2+} ion over nitrogen donor atoms. Ligands with varying substituent sizes, such as compounds **7**, **9**, and **15**, all demonstrate oxygen coordination (Figure 2, Figure S4) suggesting this preference for the oxygen donor cannot be explained by steric hindrance. A more likely explanation is the [($Tp^{Ph,Me}$)Zn] complex has a preference for the more electronegative oxygen donor atom. In addition, the coordination motif of **9** was especially surprising, as it shows coordination of the picolinic isostere is preferred over coordination by the hydroxamic acid group contained within **9**.[15] The

[($Tp^{Ph,Me}$)Zn(**9**)] complex presented here shows that suitable MBIs may be preferred even over widely used coordination motifs found in metalloenzyme inhibitors.

The MBIs containing cyclic isosteres (**17**, **18**, **19**, **20**, **21**, **23**) all coordinated through the pyridinyl nitrogen and a deprotonated heterocyclic nitrogen donor atom. The fused ring MBI **24** exhibited similar coordination as **2**, with bidentate coordination through the pyridinyl nitrogen and deprotonated triazolol oxygen. MBIs **21** and **23** resulted in a complex where a water molecule displaces one of the pyrazole arms of the $Tp^{Ph,Me}$ ligand (Figure 2). This bidentate coordination by pyrazolylborate scorpionate ligands to Zn^{2+} is uncommon and has only been observed twice crystallographically: in a homoleptic $Zn(Tp)_2$ complex,[25] and in heteroleptic ZnTp complexes with exceptional steric bulk.[26] In both of these examples an additional solvent molecule was not found coordinating the Zn^{2+} ion, as is observed in [($Tp^{Ph,Me}$)Zn(**21**)] and [($Tp^{Ph,Me}$)Zn(**23**)]. It is unlikely that the pyrazole displacement is the result of a steric clash between the exocyclic substituent of the MBIs and the substituted pyrazole ring, as the structure of [($Tp^{Ph,Me}$)Zn(**20**)] (Figure 2) shows the expected, tridentate mode of $Tp^{Ph,Me}$ binding, whilst possessing a similar exocyclic substituent. Based on these observations, the pyrazole displacement in [($Tp^{Ph,Me}$)Zn(**21**)] and [($Tp^{Ph,Me}$)Zn(**23**)] are likely due to electronic effects, although further studies are necessary to confirm this hypothesis and whether it may be relevant to the inhibition of metalloenzymes by these MBIs.

All MBIs structurally characterized as [($Tp^{Ph,Me}$)Zn] complexes exhibited a similar bidentate coordination motif. This indicates that carboxylic isostere replacement does not result in a loss of metal binding ability for these compounds. Overall, these results demonstrate that isostere replacement is an effective method for opening new chemical space for metalloenzyme inhibition.

Physicochemical Properties of MBIs.

Upon determining that MBIs retain the coordinative abilities of **1**, an evaluation of physicochemical properties was performed. The acidity (pK_a) of the acidic isostere group of each MBI was determined using UV-based or potentiometric methods (Table 1).[16,17] The MBIs exhibited a broad range of acidity constants (pK_a <1.5 to >12.5) demonstrating the ability to modulate this important physicochemical property. The compounds were further analyzed by determining the hydrophobicity (LogP) via a potentiometric method,[18] which combined with pK_a values was then used to derive the lipophilicity ($LogD_{7.4}$) at pH 7.4 (Table 1).

From the results of the physicochemical analysis of the MBIs, a wide range of pK_a, LogP, and $LogD_{7.4}$ values were achieved. In light of the wide range of pK_a values measured, (**12** vs. **23**, Table 1), it is apparent that changes in pK_a do not interfer with the ability of these MBIs to form metal complexes, as evidence by the results with [($Tp^{Ph,Me}$)Zn(MBI)] model compounds. Perhaps more important were the large variations in LogP and $LogD_{7.4}$ of the MBIs. LogP ranged from −0.6 to ~1.5 (**5** vs. **11**, Table 1) [($Tp^{Ph,Me}$)Zn(MBI)] and similarly $LogD_{7.4}$ values ranged from −3.43 to 1.54 (**23** vs. **11**, Table 1). Overall, these results show it is possible to significantly modulate physicochemical properties of the metal binding motif,

while still preserving metal coordination capabilities. The ability to independently modulate these features of a metal-binding motif suitable for drug development has not been previously demonstrated.

MBI Screening.

To assess the utility of MBIs to serve as fragments for metalloenzyme targeted FBDD, the MBIs were screened against several metalloenzymes for inhibitory activity. Endo, a dinuclear Mn^{2+}/Mg^{2+} metalloenzyme was selected as it is inhibited by picolinic acid (**1**). In contrast, the Zn^{2+} metalloenzyme hCAII was selected because it is not effectively inhibited by picolinic acid (**1**, IC50 >1 mM, unpublished data), which would therefore reveal any unexpected (and potentially off-target) activity of the MBIs. Both Endo and hCAII were screened against **1** and the MBIs at a fragment concentration of 200 μM (Figure 3).

From the screening results against Endo, approximately half of the MBIs exhibited similar inhibitory activity as picolinic acid (generally within ~20% of the activity of **1**). MBIs **3**, **5**, **8**, **11**, **12**, **13**, **16**, **18**, and **23** exhibited poorer activity (<15% inhibition at 200 μM), while **9** exhibited significantly improved activity (~96% inhibition at 200 μM). The improved activity of **9** might originate from coordination to both Mn^{2+} ions of the dinuclear Endo active site. It is possible that the hydroxamate group of **9** is engaging in bidentate coordination to one ion and the pyridine and the hydroxamate carbonyl oxygen coordinate the other (Figure S16).[27] Overall, a significant number (~50%) of MBIs exhibited comparable inhibitory activity as **1** towards Endo showing that MBIs provide versatile scaffolds for isostere replacement in metalloenzyme inhibitors.

In contrast to Endo, only three MBIs (**5**, **9**, **13**, Figure 3) exhibited any significant inhibitory activity against hCAII. Only compound **5**, which possesses a sulfonamide isostere, showed strong inhibition of hCAII (100% inhibition at 200 μM). This was unsurprising, as aryl sulfonamides are a privileged scaffold for inhibition of carbonic anhydrases.[28] Similarly, hydroxamic acids have previously been shown to inhibit hCAII,[29] which is the isostere found in compound **9**, which demonstrated weak inhibitory activity (~33% inhibition at 200 μM). Surprisingly, MBI **13** exhibited inhibitory activity (32% inhibition at 200 μM), which was unexpected as the very similar MBI **12** showed no activity. The observed lack of activity with **12** suggests that the thietane moiety of **13** is having some inhibitory effect. In general, isostere replacement did not result in an appearance of unexpected inhibitory activity against hCAII.

Overall, the screening results against Endo and hCAII, demonstrate that isostere replacement results in similar activity as **1** against different metalloenzymes. MBIs generally maintained inhibitory activity against Endo, but showed no unanticipated, emergent inhibition against hCAII. Based on these results, isostere replacement of MBPs with carboxylate groups results in MBIs that retain activity without introducing unexpected, off-target activity. These results establish MBIs as a new set of scaffolds for metalloenzyme FBDD.

CONCLUSIONS

Isostere replacement of MBPs to produce MBIs is a viable strategy for metalloenzyme inhibition for a large number of carboxylic acid isosteres. The broad range of isosteres utilized in this work, particularly some of the more exotic heterocycle isosteres, provide a novel source of metal binding functional groups not previously described in inorganic, bioinorganic, or medicinal chemistry. Without sacrificing inhibitory activity, MBIs can be used to modulate the physicochemical properties of metalloenzyme inhibitors at the metal binding warhead, which is frequently plagued with limited chemical diversity. Based on the success of these MBIs, isostere replacement holds great promise as a viable method for other functional groups found in MBPs.

Supplementary Material

Refer to Web version on PubMed Central for supplementary material.

ACKNOWLEDGMENTS

This work was supported by the National Institutes of General Medical Sciences (R01-GM098435). B.L.D. was supported by the National Institute of Health Molecular Biophysics Training Grant (T32GM008326–26). We thank Prof. Arnold Rheingold and Dr. Curtis Moore (U.C. San Diego) for assistance with crystallographic data collection and structure determination. We also thank Dr. Yongxuan Su for mass spectrometry sample analysis at The Molecular Mass Spectrometry Facility at UC San Diego.

REFERENCES

1. Patani GA; LaVoie EJ Bioisosterism: A Rational Approach in Drug Design. Chem. Rev 1996, 96, 3147–3176. [PubMed: 11848856]
2. Meanwell NA Synopsis of Some Recent Tactical Application of Bioisosteres in Drug Design. J. Med. Chem 2011, 54, 2529–2591. [PubMed: 21413808]
3. Kalgutkar AS; Scott Daniels J In Metabolism, Pharmacokinetics and Toxicity of Functional Groups: Impact of Chemical Building Blocks on ADMET; The Royal Society of Chemistry: 2010, p 99–167.
4. Lassila T; Hokkanen J; Aatsinki SM; Mattila S; Turpeinen M; Tolonen A Toxicity of Carboxylic Acid-Containing Drugs: The Role of Acyl Migration and CoA Conjugation Investigated. Chem. Res. Toxicol 2015, 28, 2292–2303. [PubMed: 26558897]
5. Pajouhesh H; Lenz GR Medicinal Chemical Properties of Successful Central Nervous System Drugs. NeuroRx 2005, 2, 541–553. [PubMed: 16489364]
6. Rautio J; Kumpulainen H; Heimbach T; Oliyai R; Oh D; Jarvinen T; Savolainen J Prodrugs: Design and Clinical Applications. Nat. Rev. Drug Discovery 2008, 7, 255–270. [PubMed: 18219308]
7. Ballatore C; Huryn DM; Smith AB Carboxylic Acid (Bio)Isosteres in Drug Design. ChemMedChem 2013, 8, 385–395. [PubMed: 23361977]
8. Lassalas P; Gay B; Lasfargeas C; James MJ; Tran V; Vijayendran KG; Brunden KR; Kozlowski MC; Thomas CJ; Smith AB, 3rd; Huryn DM; Ballatore C Structure Property Relationships of Carboxylic Acid Isosteres. J. Med. Chem 2016, 59, 3183–3203. [PubMed: 26967507]
9. Erlanson DA; Fesik SW; Hubbard RE; Jahnke W; Jhoti H Twenty Years On: The Impact of Fragments on Drug Discovery. Nat. Rev. Drug Discovery 2016, 15, 605–619. [PubMed: 27417849]
10. Cohen SM A Bioinorganic Approach to Fragment-Based Drug Discovery Targeting Metalloenzymes. Acc. Chem. Res 2017, 50, 2007–2016. [PubMed: 28715203]
11. Jacobsen JA; Fullagar JL; Miller MT; Cohen SM Identifying Chelators for Metalloprotein Inhibitors Using a Fragment-Based Approach. J. Med. Chem 2011, 54, 591–602. [PubMed: 21189019]

12. Chen AY; Thomas PW; Stewart AC; Bergstrom A; Cheng Z; Miller C; Bethel CR; Marshall SH; Credille CV; Riley CL; Page RC; Bonomo RA; Crowder MW; Tierney DL; Fast W; Cohen SM Dipicolinic Acid Derivatives as Inhibitors of New Delhi Metallo-beta-lactamase-1. J. Med. Chem 2017, 60, 7267–7283. [PubMed: 28809565]
13. Credille CV; Chen Y; Cohen SM Fragment-Based Identification of Influenza Endonuclease Inhibitors. J. Med. Chem 2016, 59, 6444–6454. [PubMed: 27291165]
14. Perez C; Li J; Parlati F; Rouffet M; Ma Y; Mackinnon AL; Chou TF; Deshaies RJ; Cohen SM Discovery of an Inhibitor of the Proteasome Subunit Rpn11. J. Med. Chem 2017, 60, 1343–1361. [PubMed: 28191850]
15. Puerta DT; Cohen SM [(TpMe,Ph)2Zn2(H3O2)]ClO4: A New H3O2 Species Relevant to Zinc Proteinases. Inorg. Chim. Acta 2002, 337, 459–462.
16. Tam KY; Takacs-Novak K Multi-Wavelength Spectrophotometric Determination of Acid Dissociation Constants: A Validation Study. Anal. Chim. Acta 2001, 434, 157–167.
17. Schonherr D; Wollatz U; Haznar-Garbacz D; Hanke U; Box KJ; Taylor R; Ruiz R; Beato S; Becker D; Weitschies W Characterisation of Selected Active Agents Regarding pK(a) Values, Solubility Concentrations and pH Profiles by SiriusT3. Eur. J. Pharm. Biopharm 2015, 92, 155–170. [PubMed: 25758123]
18. Slater B; Mccormack A; Avdeef A; Comer JEA Ph-Metric Log-P .4. Comparison of Partition-Coefficients Determined by Hplc and Potentiometric Methods to Literature Values. J. Pharm. Sci 1994, 83, 1280–1283. [PubMed: 7830244]
19. Monnard FW; Heinisch T; Nogueira ES; Schirmer T; Ward TR Human Carbonic Anhydrase II as a Host for Piano-Stool Complexes Bearing a Sulfonamide Anchor. Chem. Commun 2011, 47, 8238–8240.
20. Dowell RI; Hales NH; Tucker H Novel Inhibitors of Prolyl 4-Hydroxylase. Part 4 Pyridine-2-Carboxylic Acid Analogues with Alternative 2-Substituents. Eur. J. Med. Chem 1993, 28, 513–516.
21. Pichota A; Duraiswamy J; Yin Z; Keller TH; Alam J; Liung S; Lee G; Ding M; Wang G; Chan WL; Schreiber M; Ma I; Beer D; Ngew X; Mukherjee K; Nanjundappa M; Teo JW; Thayalan P; Yap A; Dick T; Meng W; Xu M; Koehn J; Pan SH; Clark K; Xie X; Shoen C; Cynamon M Peptide Deformylase Inhibitors of Mycobacterium Tuberculosis: Synthesis, Structural Investigations, and Biological Results. Bioorg. Med. Chem. Lett 2008, 18, 6568–6572. [PubMed: 19008098]
22. Puerta DT; Cohen SM Examination of Novel Zinc-Binding Groups for Use in Matrix Metalloproteinase Inhibitors. Inorg. Chem 2003, 42, 3423–3430. [PubMed: 12767177]
23. Jacobsen FE; Lewis JA; Cohen SM A New Role for Old Ligands: Discerning Chelators for Zinc Metalloproteinases. J. Am. Chem. Soc 2006, 128, 3156–3157. [PubMed: 16522091]
24. Sun Cao P; Sommer RD; Grice KA Structural Comparison of Suberanilohydroxamic acid (SAHA) and Other Zinc-Enzyme Inhibitors Bound to a Monomeric Zinc Species. Polyhedron 2016, 114, 344–350.
25. Kremer-Aach A; Kläui W; Bell R; Strerath A; Wunderlich H; Mootz D Cobalt as a Probe for Zinc in Metalloenzyme Model Compounds? A Comparison of Spectroscopic Features and Coordination Geometry of Four- and Five-Coordinate Complexes. Crystal and Molecular Structures of [Co(η3-TpPh)(η2-TpPh)], [(η3-TpPh)Zn(anthranilate)], and [(η3-TpPh)M(η2-acac)] (TpPh = Hydrotris(3-phenylpyrazol-1-yl)borate, acac = Pentane-2,4-dionate, and M = Zn, Co). Inorg. Chem 1997, 36, 1552–1563. [PubMed: 11669742]
26. Rombach M; Gelinsky M; Vahrenkamp H Coordination Modes of Aminoacids to Zinc. Inorg. Chim. Acta 2002, 334, 25–33.
27. DuBois RM; Slavish PJ; Baughman BM; Yun MK; Bao J; Webby RJ; Webb TR; White SW Structural and Biochemical Basis for Development of Influenza Virus Inhibitors Targeting the PA Endonuclease. PLoS Pathog. 2012, 8, e1002830. [PubMed: 22876176]
28. Supuran CT; Scozzafava A; Casini A Carbonic Anhydrase Inhibitors. Med. Res. Rev 2003, 23, 146–189. [PubMed: 12500287]
29. Di Fiore A; Maresca A; Supuran CT; De Simone G Hydroxamate Represents a Versatile Zinc Binding Group for the Development of New Carbonic Anhydrase Inhibitors. Chem. Commun 2012, 48, 8838–8840.

Synopsis Text:

Carboxylic acid isosteres of picolinic acid have been synthesized and characterized as a new class of ligand ‘warheads’ for use in metalloenzyme inhibitors. These metal-binding isosteres (MBIs) retain the ability to coordinate metal ions in a bidentate fashion, allowing for substantial variation in physiochemical properties (e.g., pK_a, logP, log$D_{7.4}$), while maintaining inhibitory activity against select metalloenzymes. These scaffolds should accelerate the development of metalloenzyme inhibitors via providing more druglike scaffolds for metal coordination.

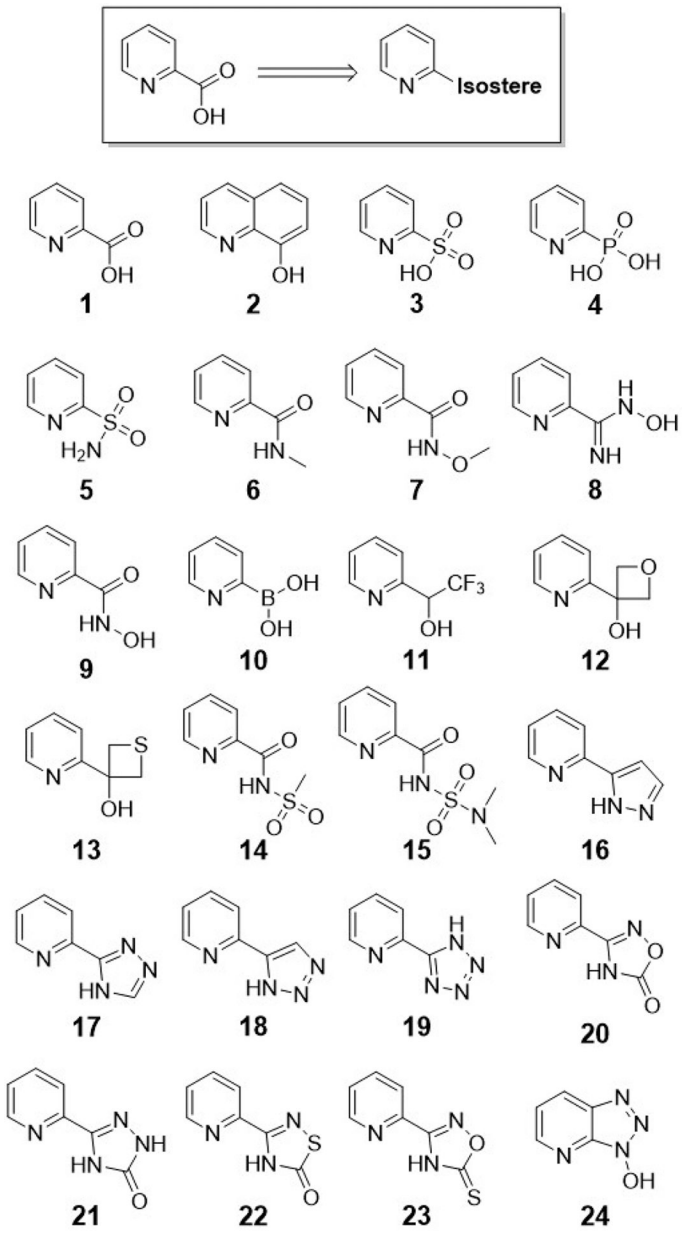

Figure 1.

Metal-binding isosteres (MBIs) of picolinic acid (1) synthesized and investigated in this study.

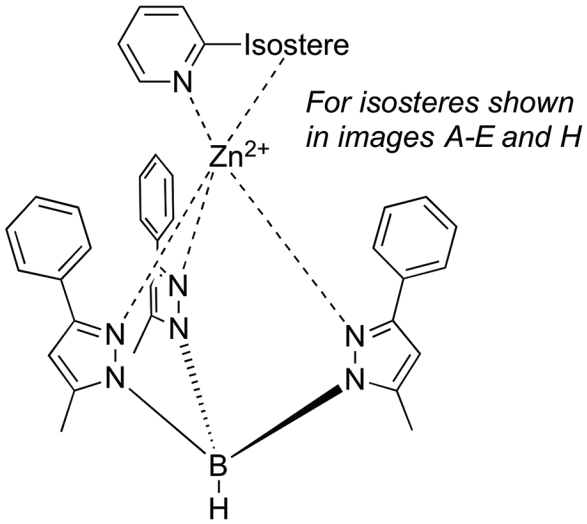

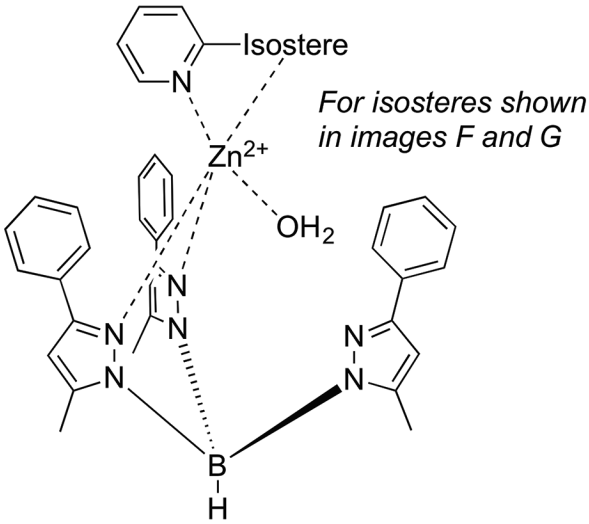

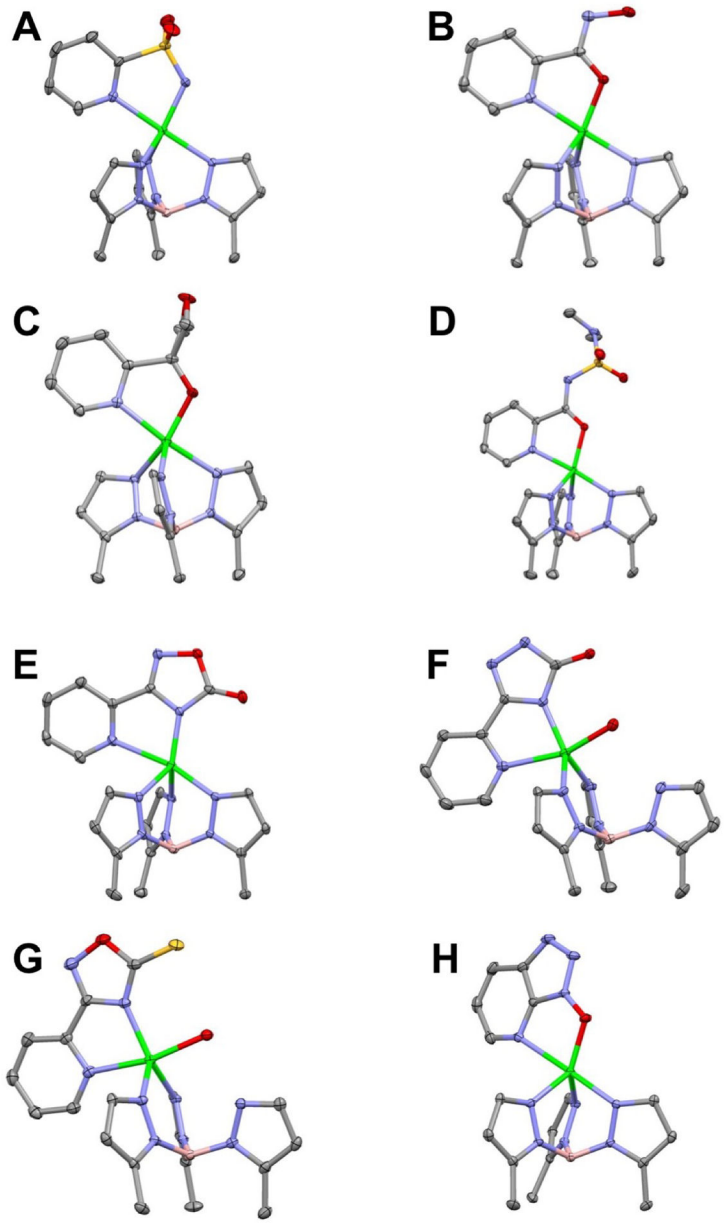

Figure 2.

Representative examples of [(Tp^{Ph,Me})Zn(MBI)] complexes shown as chemical structures (*top*) and ORTEPs (*bottom*) with atoms as 50% thermal probability ellipsoids. A: [(Tp^{Ph,Me})Zn(**5**)]. B: [(Tp^{Ph,Me})Zn(**9**)]. C: [(Tp^{Ph,Me})Zn(**12**)]. D: [(Tp^{Ph,Me})Zn(**15**)]. E: [(Tp^{Ph,Me})Zn(**20**)]. F: [(Tp^{Ph,Me})Zn(**21**)]. G: [(Tp^{Ph,Me})Zn(**23**)]. H: [(Tp^{Ph,Me})Zn(**24**)]. Hydrogen atoms and Tp^{Ph,Me} phenyl groups have been removed for clarity. Color scheme: carbon = gray, oxygen = red, nitrogen = blue, boron = pink, and zinc = green.

Compound	Endo	hCAII
1	41	<5
2	41	<5
3	12	6
4	45	<5
5	6	100
6	20	6
7	49	<5
8	14	13
9	96	33
10	22	<5
11	<5	<5
12	8	6
13	<5	32
14	31	<5
15	22	<5
16	13	10
17		12
18	<5	
19	18	<5
20	30	<5
21	39	<5
22	40	<5
23	11	<5
24	22	<5

Figure 3.

Thermoplot of screening of MBIs against Endo (200 μM) and hCAII (200 μM) with percent inhibition values included. Cells are color-coded by percent inhibition: white (<20%), yellow (20–50%), and red (51–100%). Gray cells were compounds that interfered with the assay. Percent inhibition values and standard deviations can be found in the ESI.

Table 1.

Measured physicochemical properties of picolinic acid and related MBIs.

Compound	pK_a[a]	LogP[a]	$LogD_{7.4}$
1	<1.5	<−2	<−2
5	9.30	−0.59	−0.55
6	>12.5	−0.66	−0.66
7	8.39	0.07	0.02
9	8.29	−0.37	−0.42
11	11.25	1.54	1.54
12	12.31	0.19	0.19
15	4.87	0.49	−2.04
16	>12.5	1.29	1.29
18	7.88	0.97	0.84
19	4.04	0.62	−2.72
20	4.76	0.65	−1.43
21	8.02	0.32	0.02
22	5.71	1.42	−0.21
23	3.09	0.88	−3.43

[a]All pK_a and LogP experiments yielded standard deviations <0.05.